Journal of Muscle Research and Cell Motility (2022) 43:99–111
https://doi.org/10.1007/s10974-022-09620-6

ORIGINAL PAPER

The effect of muscle length on post-tetanic potentiation of C57BL/6 and skMLCK$^{-/-}$ mouse EDL muscles

Angelos Angelidis[1] · **Rene Vandenboom**[1]

Received: 17 March 2022 / Accepted: 12 May 2022 / Published online: 30 June 2022

Abstract

Post-tetanic potentiation of fast-twitch skeletal muscle is dependent on muscle length, with greater potentiation observed at shorter compared to longer lengths. The structural effects of the primary potentiation mechanism, phosphorylation of the regulatory light chain (RLC) of myosin, are thought to explain this relationship. The purpose of these experiments was to determine whether the length-dependence of potentiation would be attenuated in the absence of RLC phosphorylation. To this end, we compared isometric twitch potentiation of mouse extensor digitorum longus (EDL) muscles with (wildtype, WT) and without (skeletal myosin light chain kinase knockout, skMLCK$^{-/-}$) phosphorylation. Force was measured at five muscle lengths (0.90 L_o, 0.95 L_o, L_o, 1.05 L_o, 1.10 L_o, where L_o refers to optimal length) prior to and following a tetanic train. In accordance with prior findings, potentiation was dependent on muscle length, with greater values observed at short (e.g., 44.3 ± 4.6% for WT, 33.5 ± 6.2% for skMLCK$^{-/-}$, at 0.90 L_o) compared to long lengths (e.g., 16.9 ± 1.3% for WT, 9.1 ± 1.8% for skMLCK$^{-/-}$, at 1.10 L_o) in both genotypes. WT muscles displayed greater potentiation compared to their skMLCK$^{-/-}$ counterparts across lengths (e.g., 16.9 ± 1.6% vs 7.3 ± 1.5% at L_o). However, the relationship between potentiation and muscle length was not different between genotypes. Thus, the alternative mechanisms of potentiation, present in the skMLCK$^{-/-}$ EDL, display a length-dependence of post-tetanic potentiation similar to RLC phosphorylation-dominant potentiation. Additional mechanisms may be required to explain the length-dependence of potentiation.

Keywords Myosin · Potentiation · Regulatory light chain · Muscle length

Introduction

Skeletal muscle contraction is facilitated by the translocation of actin thin filaments by myosin. This process is coupled to ATP hydrolysis and product release (Sweeney and Houdusse 2010; Houdusse and Sweeney 2016). In mammals, myosin-actin interactions are regulated at two levels: release of Ca^{2+} from the sarcoplasmic reticulum (SR) during excitation–contraction coupling (ECC) results in Ca^{2+} binding to troponin C (Gordon et al. 2000; Lehman 2016). Subsequent structural changes allow for the movement of tropomyosin on actin, revealing the myosin-binding sites and permitting interaction (Gordon et al. 2000; Lehman 2016). At the same time, the number of myosin heads extending from the thick filament backbone to bind to actin is regulated at the level of the thick filament; this occurs through thick filament mechanosensing (Linari et al. 2015; Fusi et al. 2016), and also likely through interfilament communication mechanisms (Woodhead & Craig 2015; Irving 2017), which remain largely unknown. In addition to these main regulatory pathways, modulatory mechanisms can also affect contraction.

A main modulatory mechanism is phosphorylation of the regulatory light chain (RLC) of myosin (Sweeney et al. 1993; Vandenboom 2017). RLC phosphorylation is mediated by skeletal Myosin Light Chain Kinase (skMLCK), which in turn is activated by a Ca^{2+}–calmodulin complex (Stull et al. 2011). This cascade is initiated during ECC, but occurs on a slower timescale than the contractile events (Stull et al. 2011). Due to the slow rates of skMLCK inactivation and RLC dephosphorylation, phosphorylation can be cumulative over multiple Ca^{2+} release events and thus act as a "molecular memory" mechanism (Stull et al. 2011). In permeabilized mammalian fibers, RLC phosphorylation results in increased Ca^{2+} sensitivity of steady-state force

✉ Angelos Angelidis
aa18lu@brocku.ca

[1] Department of Kinesiology, Centre for Bone and Muscle Health, Brock University, 1812 Sir Isaac Brock Way, St. Catharines, ON L2S 3A1, Canada

at submaximal but not maximal [Ca^{2+}] (Persechini et al. 1985; Sweeney and Stull 1986, 1990; Metzger et al. 1989; Stephenson & Stephenson 1993; Szczesna et al. 2002), as well as rate of force redevelopment at intermediate [Ca^{2+}] (Metzger et al. 1989; Sweeney and Stull 1990) (c.f. Szczesna et al. 2002). In intact skeletal muscle, RLC phosphorylation is the main mechanism of post-tetanic potentiation (PTP) (Zhi et al. 2005) i.e., the increased twitch force observed following a tetanic stimulus (Close and Hoh 1968). Extensor digitorum longus (EDL) muscles from skMLCK knockout mice (skMLCK$^{-/-}$), which do not exhibit stimulation-induced increases in RLC phosphate content, display either completely ablated (Zhi et al. 2005) or attenuated (Gittings et al. 2011; Overgaard et al. 2022) isometric PTP. The discrepancy between the initial observation of ablated PTP by Zhi et al. (2005) and the decreased PTP observed later in our lab (Gittings et al. 2011; Overgaard et al. 2022 and findings here) is likely related to the different stimulation protocols utilized. Importantly, this remnant PTP observed in the skMLCK$^{-/-}$ EDL (Zhi et al. 2005; Gittings et al. 2011, 2017; Bowslaugh et al. 2016) and other RLC-phosphorylation void models, such as wildtype (WT) mouse lumbrical muscles (Smith et al. 2013), indicates that additional mechanisms exist. Structurally, RLC phosphorylation disrupts the folded-back conformation of myosin heads on the thick filament backbone, known as the "interacting heads motif" (reviewed in Alamo et al. 2017, 2018), thus radially displacing the heads towards the thin filament (Levine et al. 1996; Yang et al. 1998; Yamaguchi et al. 2016). This has been demonstrated in isolated mammalian thick filaments (Levine et al. 1996; Yang et al. 1998) and permeabilized fibers (Yamaguchi et al. 2016), and is thought to result in enhanced probability of myosin-actin interactions, explaining the observed effects in functional studies (Levine et al. 1996; Yang et al. 1998).

Post-tetanic potentiation is inversely related to muscle or sarcomere length (Rassier et al. 1997, 1998; Rassier and MacIntosh 2000, 2002a; Rassier and Herzog 2002) (c.f. Moore and Persechini 1990). This relationship has been attributed to the aforementioned structural effects of RLC phosphorylation. Interfilament lattice spacing (i.e., the distance between thin and thick filaments) is decreased at longer sarcomere lengths (Millman 1998), and it has been proposed that this makes the displacement of the heads redundant (Yang et al. 1998; MacIntosh 2010). The phenomenon of length-dependent activation (LDA) might also explain the length-dependence of potentiation; LDA refers to the increased Ca^{2+} sensitivity observed at longer sarcomere lengths in striated muscle (Rassier et al. 1999; de Tombe et al. 2010). The mechanisms of LDA remain unclear, but likely include both the reduction in interfilament lattice spacing and structural mechanisms downstream of titin mechanosensing (Rassier et al. 1999; de Tombe et al. 2010; Williams et al. 2010, 2013; Mateja et al. 2013; Ait-Mou et al. 2016; Li et al. 2016; Zhang et al. 2017); in skeletal muscle, the latter might be related to partial thick filament activation (Reconditi et al. 2014; Fusi et al. 2016), as well as effects of other sarcomeric components like Myosin-Binding Protein-C (MyBP-C) (Reconditi et al. 2014). Thus, RLC-phosphorylation mediated increases in Ca^{2+} sensitivity would be expected to be less impactful at longer sarcomere lengths.

The length-dependence of potentiation has not been previously investigated in the context of RLC-phosphorylation independent potentiation. To this end, we utilized skMLCK$^{-/-}$ and WT mouse EDL muscles, and assessed PTP at a range of muscle lengths. As mentioned above, despite the absence of increased RLC phosphorylation following stimulation, skMLCK$^{-/-}$ EDL muscles still display a smaller amount of potentiation. We hypothesized that potentiation length-dependence would be attenuated in skMLCK$^{-/-}$ compared to wildtype muscles. In turn, this would become apparent as a significantly different pattern of length-dependence of potentiation between the two genotypes.

Methods

All experimental procedures were approved by the Brock University Animal Care and Use Committee. Wildtype mice with a C57BL/6 background (male and female, aged 10–24 weeks) were obtained from Charles River Laboratories (St. Constant, QC), while age-matched skMLCK$^{-/-}$ mice were obtained from our on-site colony (for information regarding the generation of the skMLCK$^{-/-}$ mouse see Zhi et al. 2005). Body mass was similar between genotypes (22.7 ± 1.1 g for WT, 23.9 ± 0.6 g for skMLCK$^{-/-}$, mean ± SEM) ($p > 0.05$). Prior to the initiation of an experiment, mice were anaesthetized via inhalation of isoflurane gas and euthanized by means of cervical dislocation. Subsequently, both EDL muscles were excised and attached either vertically to a jacketed organ bath of the experimental apparatus (Model 1200A, Aurora Scientific Inc., Aurora, ON), or to a resting bath, using surgical silk suture. In both cases, muscles were incubated in continuously gassed (95% O_2, 5% CO_2) Tyrode's solution (in mM: 121 NaCl, 24 $NaHCO_3$, 5 KCl, 0.34 NaH_2PO_4, 0.23MgCl, 1.8 CaCl, 5.5 D-glucose, 0.07 EDTA). Experiments were done at 25 °C, and stimulation voltage was set at 1.25 the threshold required for maximal twitch force production (25–80 V depending on the muscle). Pulse duration was 0.1 ms for all the stimuli used during the experiments. Following suspension, each muscle underwent an equilibration period (≥ 30 min), with one twitch elicited every 3 min. Data were collected (1000 Hz sampling frequency) and monitored using Aurora Scientific's 600A software (Aurora Scientific Inc., Aurora, ON).

Contractile forces (either twitch or tetanic, in mN), $+df/dt$ and $-df/dt$ (i.e., rates of force development and relaxation, respectively, in mN/ms) were determined directly from the 600A analysis function. $+Df/dt$ and $-df/dt$ refer to peak values observed during a given twitch. Time to peak tension (TPT, in ms) and half-relaxation time (½ RT, in ms) were calculated from the raw data using custom Microsoft Excel (Microsoft Corp., 2018) spreadsheets.

Determination of optimal length (L_o)

Following equilibration, doublets (3 ms spacing) were utilized to approximate optimal length for tetanic force (see Rassier and MacIntosh 2002b). An initial stimulus was given at 5 mN passive tension and subsequently at 0.5 mN intervals above and below this value, with 20 s between successive doublets. When maximal active force was detected (total force—passive force prior to initiation of stimulation), muscle length was measured using digital vernier calipers and defined as optimal length (L_o). In cases where force values were similar between lengths, the shorter length was selected. Baseline twitch force at L_o was then measured (mean of two twitches).

Experimental protocol

Post-tetanic potentiation (PTP) was assessed at five relative muscle lengths (0.90 L_o, 0.95 L_o, L_o, 1.05 L_o, 1.10 L_o). The experimental protocol included an initial 200-s isometric twitch pacing period (one twitch every 20 s). For each contractile property, the mean of the last 3 twitches of the pacing period was considered as the "Pre" (i.e., unpotentiated) value. Thirty s after the pacing period, a conditioning stimulus was administered, consisting of 4 × 100 Hz, 400 ms isometric tetani within a 20-s window. Importantly, the CS was done at the same muscle length as the prior and following twitches, and not always at L_o. Peak tetanic force (P_o) was defined as the highest active force value (total force—passive force prior to initiation of stimulation) recorded during the CS, at each length. Finally, at 10 and 30 s following the 20-s CS window, twitches were elicited to assess potentiation. Values from these twitches were considered as the "Post 10" and "Post 30" values respectively, for all contractile properties. To assess changes following the CS, post values were divided by pre values and expressed as % change (i.e., Post/Pre × 100%). Each muscle underwent this protocol at every experimental length in a randomized order, with 20 min of rest between lengths to allow for the effects of potentiation and fatigue to dissipate (see Fig. 1 for a visual summary of the main experimental protocol). After the end of this process, muscles were taken to L_o and went through a 30-min rest period, with one twitch elicited every 3 min. Subsequently, twitch force was assessed again (mean of two twitches) and compared to baseline values. Muscles were excluded from analysis if active force had declined by > 5%.

Statistical analysis

Body mass was compared between genotypes using an independent samples t-test. A two-way mixed ANOVA was utilized for P_o, with muscle length and genotype as the factors. For twitch force (P_t) and all other contractile properties as well as their potentiation values, three-way mixed ANOVAs were used with muscle length, genotype and time as the factors. Data were assessed for existence of outliers through boxplot inspection. Outliers detected

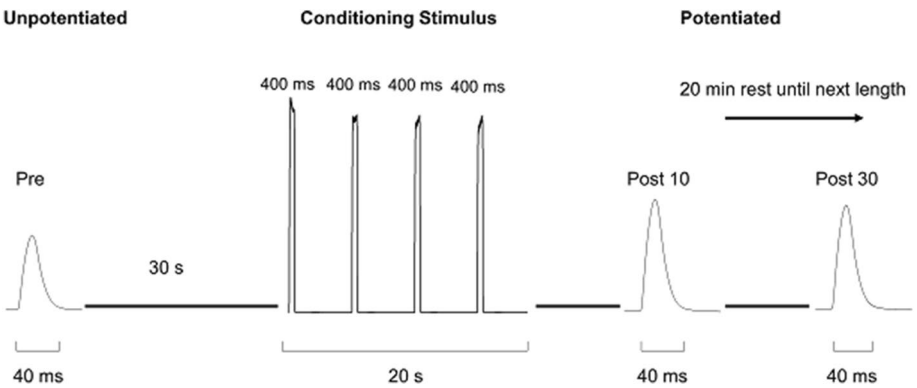

Fig. 1 Overview of the main experimental protocol. Initially, there was a 200 s isometric twitch pacing period (1/20 s) (i.e., Pre). Thirty seconds following the end of pacing, a conditioning stimulus (CS) was elicited, comprising 4 × 100 Hz, 400 ms isometric tetani within a 20 s window. Isometric twitches were elicited 10 (Post 10) and 30 (Post 30) s after the CS 20-s window to assess potentiation. Each muscle underwent this protocol at five relative muscle lengths (0.90 L_o, 0.95 L_o, L_o, 1.05 L_o, 1.10 L_o) in a randomized order, with 20 m of rest between successive lengths. Please note that the CS and resting period took place at the same relative muscle length as the Pre and Post twitches in each case, and not always at L_o. Pre values for each measured variable were defined as the mean of the last three twitches of the pacing period, in each case

were included in the final analyses, as no differences were apparent regarding the significance of interactions and main effects when tests were repeated without them. Normality was evaluated using Shapiro–Wilk's test in all cases. Homogeneity of variance for the between-subjects factor was assessed using Levene's test. Both for normality and homogeneity of variance, violations were noted in some cells of the design for all measured dependent variables. These were always in a minority of the cells, and the decision was made to carry on with the analyses. The tables of the assumption tests are provided in Online Resource 1, so the interested reader can assess our decisions. Mauchly's test of sphericity was used where appropriate and a Greenhouse–Geisser correction was applied in cases where the assumption was violated. Post-hoc pairwise comparisons with Bonferroni corrections, or polynomial contrasts for trend analysis were utilized to further evaluate significant simple main effects or main effects. For each significant trend (linear, quadratic, cubic or higher order), its sum of squares was divided by the sum of squares of the total observed trend in each case, to assess the percentage of variance it could explain. Multiple simple main effect testing within a given interaction was also controlled for with Bonferroni corrections. Significance level was $\alpha = 0.05$ and data are reported as mean ± SEM (standard error of the mean). All analyses were done in IBM SPSS Statistics for Windows, versions 27 and 28 (IBM Corp., Armonk, NY, USA).

Results

P_o and unpotentiated (i.e., Pre) P_t were not significantly different between WT and skMLCK$^{-/-}$ muscles at any muscle length (both $p > 0.05$) (e.g., Pre P_t at L_o was 51.3 ± 3.4 mN for WT and 48.9 ± 3.7 mN for skMLCK$^{-/-}$). In contrast, while both genotypes exhibited PTP, WT Post 10 and Post 30 P_t were significantly greater compared to skMLCK$^{-/-}$ values at every muscle length (both $p < 0.001$) (e.g., 16.9 ± 1.6% potentiation for WT compared to 7.3 ± 1.5% for skMLCK$^{-/-}$ muscles at L_o, at Post 10). In both genotypes, Post 10 P_t values were greater than Post 30 P_t values, again at every muscle length (all $p < 0.001$) (e.g., at L_o, Post 10 potentiation was 16.9 ± 1.6% for WT and 7.3 ± 1.5% for skMLCK$^{-/-}$, while Post 30 potentiation was 13.9 ± 1.4% for WT and 2.77 ± 1.2% for skMLCK$^{-/-}$). All the above data are summarized in Table 1.

Length-dependence of potentiation

PTP was dependent on muscle length in the WT muscles ($p < 0.001$ at both Post 10 and Post 30). For example, PTP was 44.3 ± 4.6% at 0.9 L_o compared to 16.9 ± 1.3% at 1.10 L_o, at Post 10. This was also observed in the skMLCK$^{-/-}$ muscles ($p < 0.001$ at both Post 10 and Post 30); PTP was 33.5 ± 6.2% at 0.9 L_o compared to 9.1 ± 1.8% at 1.10 L_o, at Post 10 (see Table 1 and Fig. 2) Contrary to our initial hypothesis, the pattern of potentiation length-dependence was not significantly different between genotypes, ($p > 0.05$ for the muscle length x genotype x time and muscle length x

Table 1 Summary force data for WT (top, n = 11) and skMLCK$^{-/-}$ (bottom, n = 12) mouse EDL muscles

Condition	Wildtype				
	Muscle length				
	0.90	0.95	1.00	1.05	1.10
Pre	36.7 ± 3.3	47.6 ± 3.6	51.3 ± 3.4	49.3 ± 3.5	45.0 ± 3.3
Post 10	52.0 ± 3.7*†	56.8 ± 3.9*†	59.8 ± 3.8*†	58.0 ± 3.9*†	52.5 ± 3.8*†
Post 30	49.5 ± 3.6*	55.0 ± 3.8*	58.3 ± 3.7*	56.8 ± 3.8*	51.7 ± 3.7*
P_o	180.3 ± 12.1	198.7 ± 12.7	211.7 ± 13.1	199.2 ± 12.9	179.2 ± 12.9
Condition	skMLCK$^{-/-}$				
	Muscle length				
	0.90	0.95	1.00	1.05	1.10
Pre	32.9 ± 3.1	45.2 ± 3.3	48.9 ± 3.7	47.4 ± 3.9	41.1 ± 4.1
Post 10	42.1 ± 3.2†	49.9 ± 3.1†	52 ± 3.5†	51.5 ± 3.7†	44.3 ± 4.0†
Post 30	38.9 ± 3.1	47.4 ± 3.1	49.9 ± 3.4	49.3 ± 3.7	42.8 ± 3.9
P_o	180.3 ± 17.8	210.8 ± 18.5	224.1 ± 20.4	217.2 ± 20.3	187.1 ± 18.8

Absolute values for twitch force (P_t, in mN) are presented for all relative muscle lengths (L/L_o), at Pre, Post 10 and Post 30. Absolute tetanic force values (P_o, in mN) at all relative muscle lengths are also displayed. Values are mean ± SEM. *Significantly different than skMLCK$^{-/-}$ at the same time point and muscle length ($p < 0.05$).†Significantly different than corresponding value at Post 30 within genotype ($p < 0.05$)

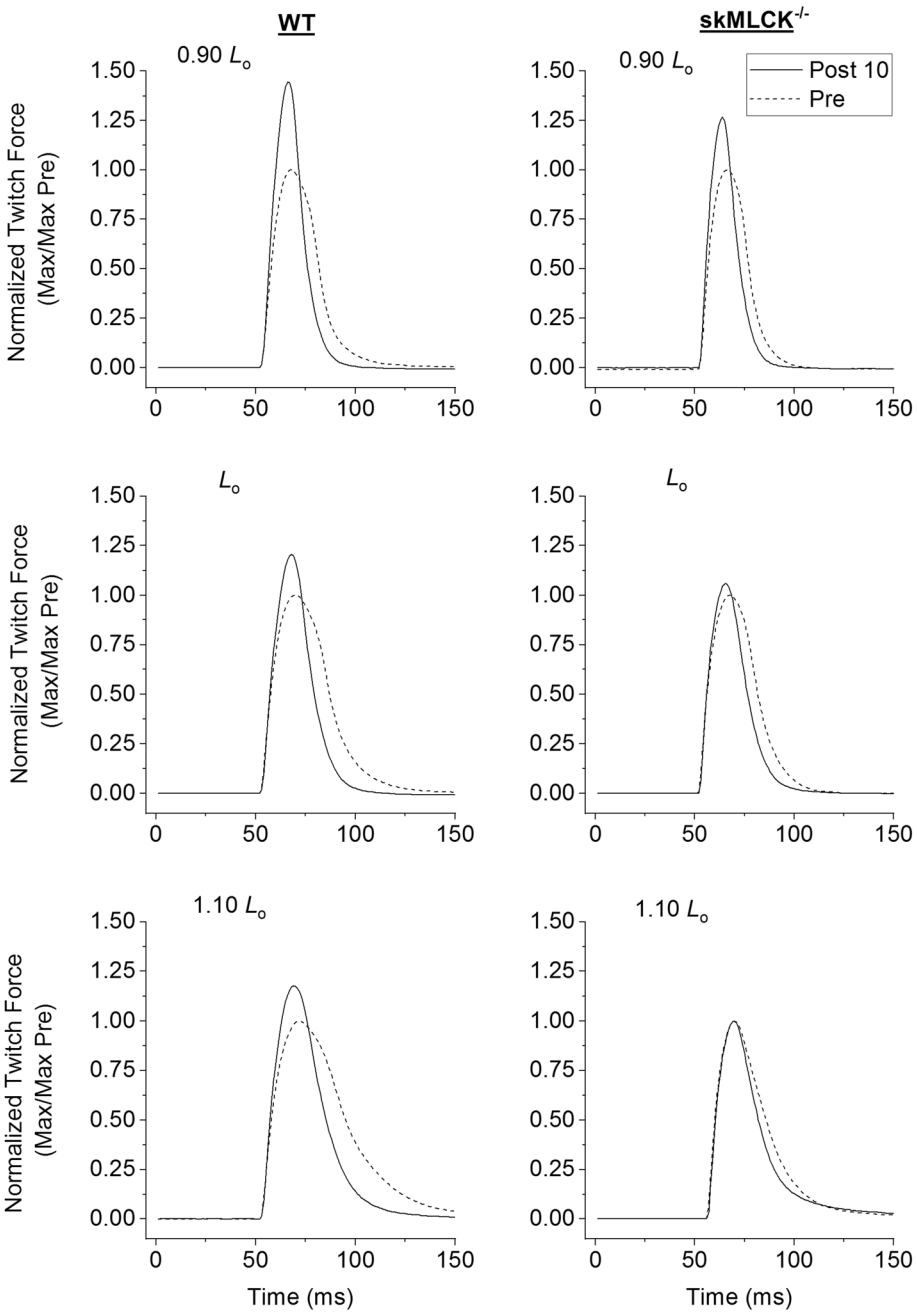

Fig. 2 Representative twitch traces from WT (left) and skMLCK$^{-/-}$ (right) mouse EDL muscles, at 0.90 L_o (top), L_o (middle) and 1.10 L_o (bottom). Post 10 twitches (*solid lines*) are superimposed on Pre twitches (*dotted lines*) to demonstrate potentiation. Force is normalized to Pre maximum values in each case. Potentiation was greater in WT muscles at every muscle length. In both genotypes, potentiation was greater at 0.90 L_o compared to the other two lengths shown

genotype interactions) (see Fig. 3). Additionally, trend analysis indicated that this pattern was similar between Post 10 and Post 30, and not distinctly linear; for example, at Post 10, there were significant linear, quadratic and cubic trends (all $p < 0.001$), which could explain 55.6%, 34.4% and 9.8% of the observed variance in potentiation with muscle length, respectively. These data are presented in Table 2.

Force development and relaxation kinetics

Unpotentiated (i.e., Pre) + dF/dt was not significantly different between genotypes at any length ($p > 0.05$) (e.g., 6.3 ± 0.4 mN/ms for WT and 6.3 ± 0.3 mN/ms for skMLCK$^{-/-}$ at L_o). Post 10 and Post 30 values were significantly increased compared to Pre values for both genotypes at every length (all $p < 0.001$), but were significantly greater for WT muscles at both timepoints and at all lengths ($p = 0.014$ for Post 10 and $p = 0.007$ for Post 30) (e.g., 17.5 ± 1.7% potentiation for WT and 10.6 ± 1.6% potentiation for skMLCK$^{-/-}$ at L_o, at Post 10) (Fig. 4). -DF/dt, while also similar between genotypes at Pre across lengths ($p > 0.05$) (e.g., -2.8 ± 0.2 mN/ms for WT and -2.6 ± 0.3 mN/ms for skMLCK$^{-/-}$ at L_o), was increased to the same extent ($p > 0.05$) in both WT and skMLCK$^{-/-}$ muscles at both Post 10 and Post 30,

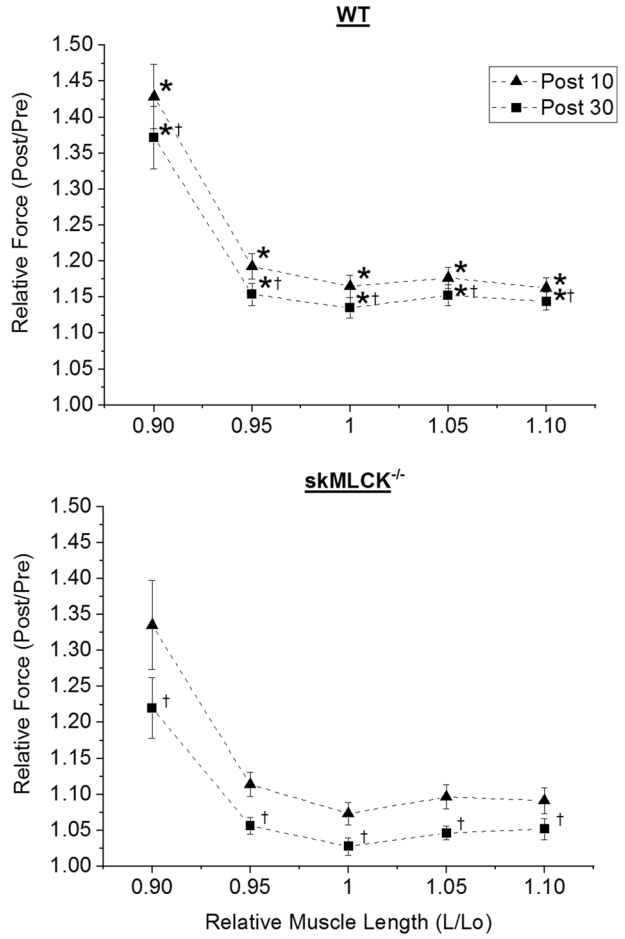

Fig. 3 Relative force (i.e., potentiation)—relative muscle length relationship for WT (top, n = 11) and skMLCK$^{-/-}$ (bottom, n = 12) mouse EDL muscles. WT values were significantly greater than skMLCK$^{-/-}$ values at both timepoints and at every muscle length. For both genotypes, Post 10 values (*triangles*) > Post 30 values (*squares*) at every muscle length. The length-dependence of potentiation was not different between genotypes (time × muscle length × genotype and muscle length × genotype interactions were not statistically significant). Additionally, potentiation length-dependence was similar between Post 10 and Post 30, as indicated by trend analysis (see Table 2). Error bars represent SEM. *Significantly different than skMLCK$^{-/-}$ at the same time point and muscle length, $p < 0.05$, †Significantly different than corresponding Post 10 value within genotype, $p < 0.001$

again at all lengths (all $p < 0.001$) (e.g., 28.9 ± 4.3% potentiation for WT and 40.7 ± 5.7% for skMLCK$^{-/-}$ at L_o, at Post 10) (Fig. 5). ½ RT was not different at Pre between WT and skMLCK$^{-/-}$ muscles at any length ($p > 0.05$) (e.g., 13.7 ± 0.5 ms for WT and 14 ± 0.4 ms for skMLCK$^{-/-}$ at L_o). Following the CS, it was decreased at both Post 10 and Post 30, with no significant differences between genotypes (both $p > 0.05$), again at every length (all $p < 0.001$) (e.g., 11 ± 0.3 ms for WT and 9.7 ± 0.4 ms for skMLCK$^{-/-}$ at L_o, at Post 10) (Fig. 6). Pre TPT was significantly greater at every length in WT muscles (main effect of genotype, $p < 0.05$) (e.g., 17.1 ± 0.3 ms for WT and 16.6 ± 0.3 ms for skMLCK$^{-/-}$ at L_o). At Post 10 and Post 30, it was decreased in both genotypes (all $p < 0.001$) and values remained significantly higher for WT muscles at all lengths (e.g., 16.1 ± 0.2 ms for WT and 15 ± 0.3 ms for skMLCK$^{-/-}$ at L_o, at Post 10) (Fig. 7).

The length-dependence of force kinetics properties was assessed through trend analysis. + *D*f/*d*t displayed a curvilinear relationship with muscle length, with values decreasing above and below L_o at all timepoints (quadratic trend could explain 94.3%, 97.5% and 99.7% of the total variance at Pre, Post 10 and Post 30, respectively; all $p < 0.001$) (Table 3); − *d*F/*d*t was maximal at 0.95 L_o and decreased above and below it, both before and after the CS. The − *d*F/*d*t—muscle length relationship was dominated by linear trends at all timepoints (linear trend could explain 74.8%, 92.2% and 90.2% of the total variance at Pre, Post 10 and Post 30, respectively; all $p < 0.001$) (Table 4). ½ RT and TPT increased with increasing muscle length, and this relationship was similar at all time points. For ½ RT, linear trends could explain 74.8%, 97.3% and 97% of the total variance at Pre, Post 10 and Post 30, respectively (all $p < 0.001$) (Table 5), while for TPT, there was no significant time x muscle length interaction ($p > 0.05$) and at all timepoints the linear trend could explain 99.4% of the total variance ($p < 0.001$) (Table 6).

Discussion

The main finding of this study was that the length-dependence of post-tetanic potentiation was not significantly different between WT and skMLCK$^{-/-}$ mouse EDL muscles. Previous findings in rat gastrocnemius in situ (Rassier et al. 1997; 1998; Rassier and MacIntosh 2000) and mouse EDL fiber bundles in vitro (Rassier and Herzog 2002; Rassier and MacIntosh 2002a) have consistently demonstrated that both PTP and staircase potentiation are dependent on muscle or sarcomere length, with potentiation diminishing as length is increased (c.f. Moore and Persechini 1990). However, all previous works have utilized wildtype models, and the length-dependence of RLC-phosphorylation independent potentiation had not been explored. Here, using skMLCK$^{-/-}$ EDL muscles we demonstrated that even though the absence of RLC phosphorylation results in lower potentiation magnitudes across the examined range of muscle lengths, it does not appear to alter its length-dependence, at least under the experimental conditions utilized. This finding extends prior knowledge on the alternative mechanisms of PTP, and provides additional information regarding potentiation length-dependence in general. Although we did not directly assess RLC phosphorylation here, between-genotype differences at rest and following conditioning stimuli

Table 2 Trend analysis table for relative force (i.e., potentiation)

Relative force (post/pre)		
Time × muscle length – F: 22.646*	Post 10 – F: 47.503*	Post 30 – F: 44.893*
% variance accounted	Post 10	Post 30
Linear	55.62%*	50.18%*
Quadratic	34.40%*	39.61%*
Cubic	9.85%*	10%*
4th order	NS	NS

The ANOVA F-values are presented for the time x muscle length interaction as well as the simple main effect of muscle length at each time point. Trend components of the polynomial contrast analysis (linear, quadratic, cubic, 4th order) are displayed as percentage of variance they can explain. Values are presented for Post 10 and Post 30. *$p < 0.001$, NS = non-significant

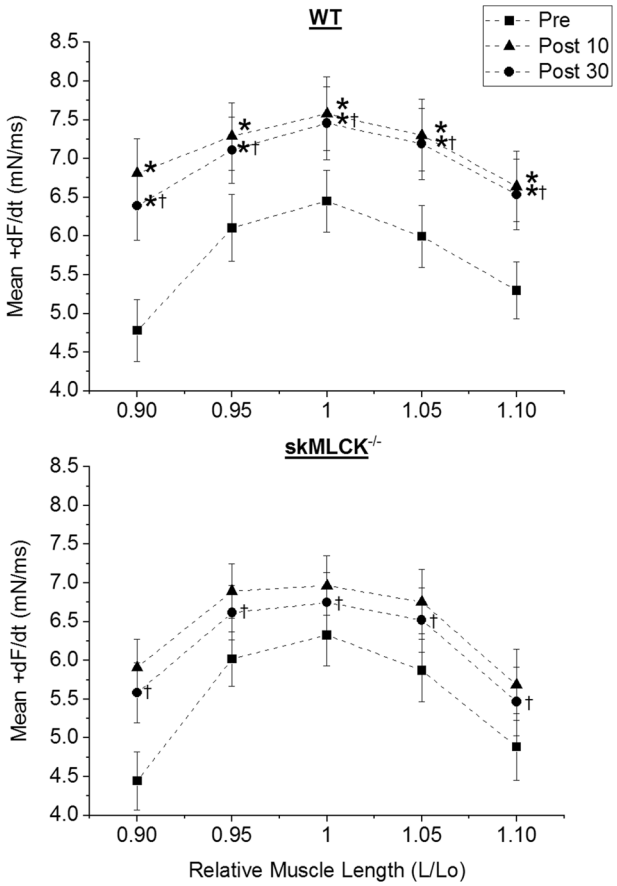

Fig. 4 +*d*F/*d*t–relative muscle length relationship for WT (top, n = 11) and skMLCK$^{-/-}$ (bottom, n = 12) mouse EDL muscles. Unpotentiated values were not significantly different between genotypes ($p > 0.05$). Post 10 ($p = 0.014$) and Post 30 ($p = 0.007$) values were significantly greater in WT compared to skMLCK$^{-/-}$ muscles, at every muscle length. In addition, within each genotype, Post 10 values (*triangles*) > Post 30 values (*circles*) > Pre values (*squares*) at every muscle length (all $p < 0.001$). Error bars represent SEM. *Significantly different than skMLCK$^{-/-}$ at the same time point and muscle length, $p < 0.05$, †Significantly different than corresponding Post 10 value within genotype, $p < 0.001$

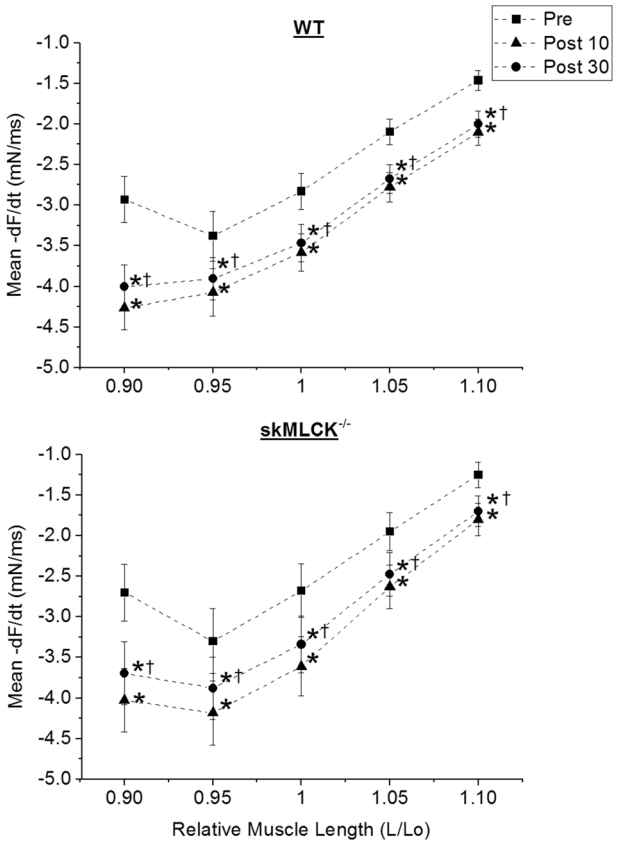

Fig. 5 – *d*F/*d*t—relative muscle length relationship for WT (top, n = 11) and skMLCK$^{-/-}$ (bottom, n = 12) mouse EDL muscles. There were no significant differences between genotypes at any time point and muscle length ($p > 0.05$). At every muscle length, Post 10 values (*triangles*) < Post 30 values (*circles*) < Pre values (*squares*) (all $p < 0.001$). Error bars represent SEM. *Significantly different than corresponding Pre value within genotype, $p < .001$, †Significantly different than corresponding Post 10 value within genotype, $p < 0.001$

similar to the one used in the current study have been documented repeatedly by our lab (Gittings et al. 2011, 2016, 2018; Bowslaugh et al. 2016; Bunda et al. 2018; Fillion et al. 2019; Morris et al. 2018). SkMLCK$^{-/-}$ EDL muscles

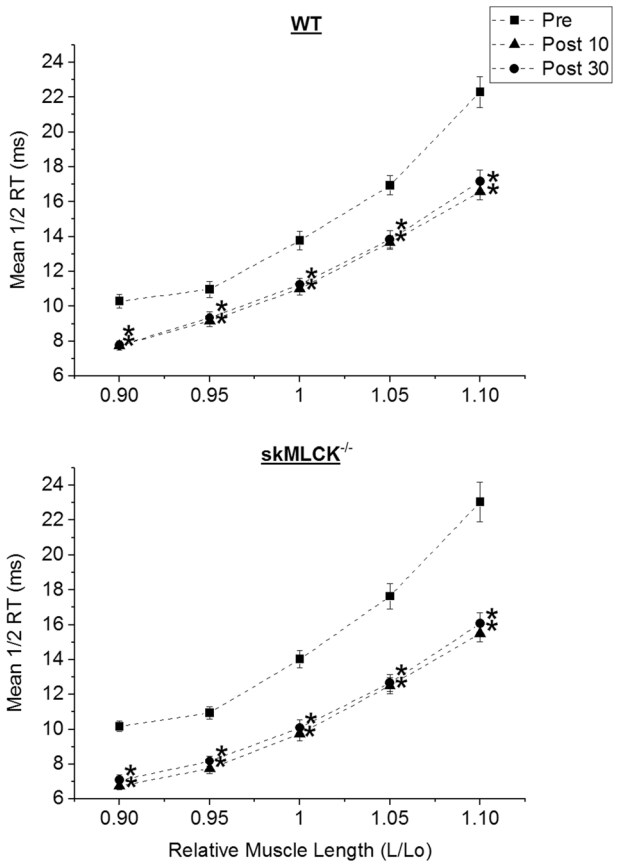

Fig. 6 Half-relaxation time (½ RT)–relative muscle length relationship for WT (top, n = 11) and skMLCK$^{-/-}$ (bottom, n = 12) mouse EDL muscles. There were no significant differences between genotypes at any time point or muscle length. Post 10 values (*triangles*) and Post 30 values (*circles*) were significantly different than Pre values (*squares*) at every muscle length (all $p < 0.001$), but they were not significantly different from each other (all $p > 0.05$). Error bars represent SEM. *Significantly different than Pre value at the same muscle length, $p < 0.001$

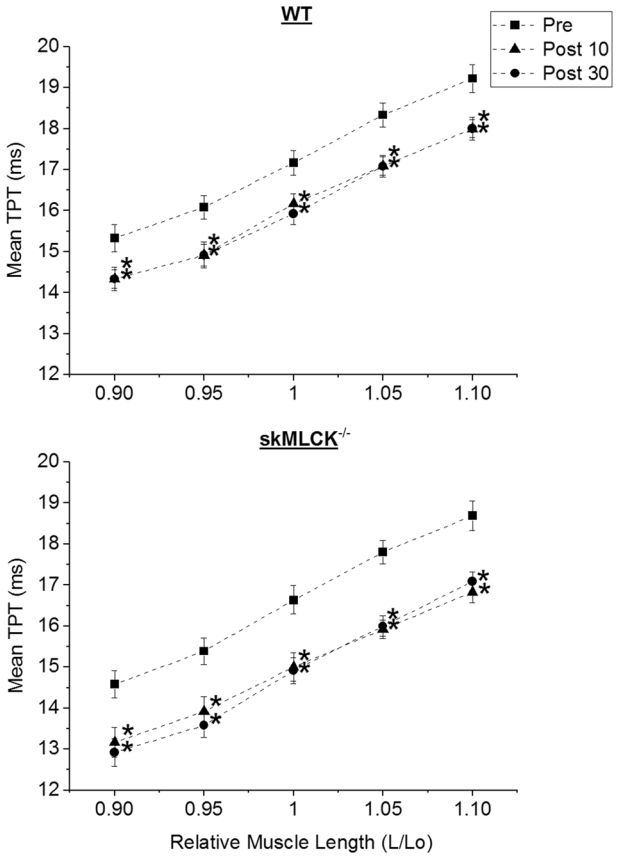

Fig. 7 Time to peak tension (TPT)–relative muscle length relationship for WT (top, n = 11) and skMLCK$^{-/-}$ (bottom, n = 12) mouse EDL muscles. WT values were significantly greater than skMLCK$^{-/-}$ values at all time points and muscle lengths (main effect of genotype: $p < 0.05$). Within each genotype, Post 10 values (*triangles*) and Post 30 values (*circles*) were significantly greater than Pre values (*squares*) at every muscle length (all $p < .001$) but they were not significantly different from each other (all $p > 0.05$). Error bars represent SEM. *significantly different than Pre within genotype, $p < 0.001$

consistently display reduced resting RLC phosphate content compared to WT muscles (e.g., Gittings et al. 2011; Bunda et al. 2018), and an absence of post-stimulation increases. In contrast, WT muscles typically display 2–4fold increases post-CS compared to baseline (e.g., Gittings et al. 2011, 2016). A difference between these data and our current experiments is that here we included conditioning stimuli at varying muscle lengths instead of L_o. However, past findings in rat gastrocnemius indicate that RLC phosphorylation is not significantly different across lengths (0.90 L_o, L_o, 1.10 L_o), at least following a staircase protocol (Rassier et al. 1997) (c.f. Moore and Persechini 1990).

The similar length-dependence of potentiation in the presence and absence of RLC phosphorylation is not readily explainable. Two main alternative potentiation mechanisms have been proposed; increased resting Ca^{2+} following stimulation (Smith et al. 2013, 2014), and S-glutathionylation of troponin-I, which increases calcium sensitivity of steady-state force in permeabilized fast, but not slow rat fibers (Mollica et al. 2012; Dutka et al. 2017). These mechanisms may interact with LDA in a currently unknown manner, and thus, regardless of the underlying mechanism, potentiation length dependence might simply be due to a ceiling effect of Ca^{2+} sensitivity at longer sarcomere lengths, as has been proposed before for RLC-phosphorylation dominant potentiation (Rassier et al. 1998; Rassier and MacIntosh 2000, 2002a; Rassier and Herzog 2002). However, if this were the case, a different length-potentiation relationship would be expected for the skMLCK$^{-/-}$ muscles since the magnitude of RLC-phosphorylation independent potentiation is smaller. Potentiation mechanisms might interact with both thin- and thick-filament related mechanisms of enhanced activation at longer sarcomere lengths (de Tombe et al. 2010; Mateja et al. 2013; Reconditi et al. 2014; Ait-Mou et al. 2016; Li

Table 3 Trend analysis table for + *d*F/*d*t

+ *d*F/*d*t			
Time × muscle length – F: 29.359*	Pre – F: 47.694*	Post 10 – F: 23.817*	Post 30 – F: 24.138*
% variance accounted	Pre	Post 10	Post 30
Linear	NS	NS	NS
Quadratic	94.31%*	97.57%*	99.76%*
Cubic	2.5%*	NS	NS
4th order	NS	NS	NS

The ANOVA F-values are presented for the time x muscle length interaction as well as the simple main effect of muscle length at each time point. Trend components of the polynomial contrast analysis (linear, quadratic, cubic, 4th order) are displayed as percentage of variance they can explain. Values are presented for Pre, Post 10 and Post 30. *p < 0.001, NS = non-significant

Table 4 Trend analysis table for – *d*F/*d*t

– *d*F/*d*t			
Time × muscle length – F: 24.869*	Pre – F: 71.892*	Post 10 – F: 143.961*	Post 30 – F: 126.776*
% variance accounted	Pre	Post 10	Post 30
Linear	74.85%*	92.28%*	90.22%*
Quadratic	19.04%*	6.5%*	8.42%*
Cubic	5.78%*	1.16%*	1.28%
4th order	NS	NS	NS

The ANOVA F-values are presented for the time × muscle length interaction as well as the simple main effect of muscle length at each time point. Trend components of the polynomial contrast analysis (linear, quadratic, cubic, 4th order) are displayed as percentage of variance they can explain. Values are presented for Pre, Post 10 and Post 30. *p < 0.001, NS = non-significant

Table 5 Trend analysis table for ½ RT

½ RT			
Time × muscle length – F: 32.821*	Pre – F: 267.395*	Post 10 – F: 576.818*	Post 30 – F: 317.889*
% variance accounted	Pre	Post 10	Post 30
Linear	74.85%*	97.35%*	97%*
Quadratic	19.04%*	2.39%	2.97%
Cubic	NS	NS	NS
4th order	0.15%**	NS	NS

The ANOVA F-values are presented for the time x muscle length interaction as well as the simple main effect of muscle length at each time point. Trend components of the polynomial contrast analysis (linear, quadratic, cubic, 4th order) are displayed as percentage of variance they can explain. Values are presented for Pre, Post 10 and Post 30. *p < 0.001, **p < 0.05, NS = non-significant

et al. 2016; Zhang et al. 2017), as well as with the effects of spatial changes of the myofilament lattice on unitary actin-myosin interactions (Williams et al. 2010, 2013). As an example, thick filaments become partially activated at long sarcomere lengths in skeletal muscle (Reconditi et al. 2014; Fusi et al. 2016), and interactions of MyBP-C with the thin filaments might be lost (Reconditi et al. 2014). Both these factors could interact with RLC phosphorylation and/or other potentiation mechanisms and result in less potentiation at longer sarcomere lengths. Nevertheless, details regarding the molecular underpinnings of the alternative potentiation mechanisms and LDA are lacking, and any proposed model can currently only be speculative. On the other hand, the fact that potentiation is enhanced at short sarcomere lengths may be related both to increased interfilament lattice spacing (Millman 1998), as has been proposed before (Levine et al. 1996; Yang et al. 1998), and to the inhibited Ca^{2+} release at short sarcomere lengths that has been observed in mammalian skeletal muscle (Rassier and Minozzo 2016). However, the latter has only been seen with high-frequency stimulation, and it is unclear whether this effect could somehow influence PTP. As with long sarcomere lengths, changes in

Table 6 Trend analysis table for TPT

TPT
Main effect: muscle length F: 242.568*
% variance accounted
Linear: 99.46%*
Quadratic: NS
Cubic: 0.37%**
4th order: NS

The ANOVA F-value is presented for the main effect of muscle length. Trend components of the polynomial contrast analysis (linear, quadratic, cubic, 4th order) are displayed as percentage of variance they can explain. *p < 0.001, **p < 0.05, *NS* non-significant

lattice spacing at short sarcomere lengths and consequent effects on unitary myosin-actin interactions (Williams et al. 2010, 2013) could also be a factor in the length-dependence of potentiation.

Our findings for force kinetics are in agreement with prior literature, both regarding the influence of muscle length (Wallinga-de Jonge et al. 1980; Rassier et al. 1997; Rassier and MacIntosh 2002b) and in relation to genotype differences prior to and following the CS (Vandenboom 2017). The greater post-tetanic increase in + *d*F/*d*t in WT compared to skMLCK$^{-/-}$ muscles has been previously observed in our lab for concentric twitches (Gittings et al. 2016) and may be a direct effect of RLC phosphorylation, parallel to increased force (Vandenboom 2017). The current findings complement earlier observations of correlations between post-tetanic increases in isometric + *d*F/*d*t and RLC phosphate content in WT mouse EDL (Vandenboom et al. 1995, 1997), and of RLC phosphorylation-mediated increases in rate of force redevelopment (i.e., k_{tr}) in permeabilized mammalian fibers (Metzger et al. 1989; Sweeney and Stull 1990). The enhanced + *d*F/*d*t was accompanied by a slight, but significant decrease in TPT in both genotypes. Notably, TPT values were significantly greater in WT muscles both prior to, and following the CS. The reason for this difference is unknown, but it has been previously observed in our lab (Bunda et al. 2018). In regard to − *d*F/*d*t, it is known that the post-tetanic increase of twitch relaxation rate does not appear to be related to RLC phosphorylation, as this effect has been observed in mouse lumbrical muscles, which display potentiation without phosphorylation (Smith et al. 2013, 2014). Here, this observation has been recapitulated, as − *d*F/*d*t was increased to the same extent in both genotypes following the CS. Similarly, ½ RT was decreased post-CS with no significant differences between genotypes, in accordance with past findings (Gittings et al. 2011). The decreased relaxation time is likely related to the increased − *d*F/*d*t in both genotypes, the mechanisms of which remain unknown (Vandenboom 2017).

Limitations

It is known that active force calculation using the traditional method (total force—passive force prior to stimulation initiation, used here) might be problematic in fixed-end contractions, due to internal sarcomere shortening (MacIntosh and MacNaughton 2005; see MacIntosh 2017 for a review). Specifically, in whole muscle preparations sarcomeres are able to pull on in-series elastic components of the experimental apparatus and tendon, and thus passive tension at the peak of force production would be lower than prior to its initiation (MacIntosh 2017). Sarcomere or fascicle length measurements can be used to control for this change (MacIntosh and MacNaughton 2005; de Tombe and ter Keurs 2016), but unfortunately were not available here. This difference in active force calculation can result in effects that are pronounced at long muscle lengths, where passive tension is high: underestimation of active force, overestimation of potentiation due to force relaxation over time (i.e., passive tension would become progressively lower giving the impression of greater force increase than actually occurred) and potential influence of shortening-induced force depression (MacIntosh 2017). While this makes mechanistic interpretation of our findings more difficult, it is not yet clear exactly what the implications of internal shortening are at the molecular level (e.g., MacDougall et al. 2020). Regardless, our findings can be compared to existing potentiation length-dependence literature, as previous works also utilized the traditional method to calculate active force.

Conclusion

The pattern of potentiation length-dependence does not differ significantly in the presence and absence of RLC phosphorylation, with potentiation being greater at short compared to long muscle lengths. While the current findings are not sufficient for a mechanistic interpretation of this similarity, they provide additional information regarding the alternative mechanisms of potentiation. Further work is necessary to understand how potentiation without RLC phosphorylation is facilitated at the molecular level, and how these mechanisms interact with sarcomere length, as well as with RLC phosphorylation when it is present.

Supplementary Information The online version contains supplementary material available at https://doi.org/10.1007/s10974-022-09620-6.

Acknowledgements This study was supported through funds provided by the Natural Sciences and Engineering Research Council (NSERC) of Canada (2019-05122) to R.V. All graphs were created using OriginPro, Version 2021 (OriginLab Corporation, Northampton, MA, USA).

Author contributions Conceptualization: AA, RV; Methodology: AA, RV; Investigation: AA; Formal Analysis: AA; Writing—Original Draft: AA; Writing—Review and Editing: AA, RV; Funding Acquisition: RV; Supervision: RV.

Data availability The data that support the findings of this study are available from the corresponding author on reasonable request.

Declarations

Conflict of interest The authors declare that they have no conflict of interest.

References

Ait-Mou Y, Hsu K, Farman GP, Kumar M, Greaser ML, Irving TC, De Tombe PP (2016) Titin strain contributes to the Frank–Starling law of the heart by structural rearrangements of both thin- and thick-filament proteins. Proc Natl Acad Sci USA 113(8):2306–2311. https://doi.org/10.1073/pnas.1516732113

Alamo L, Koubassova N, Pinto A, Gillilan R, Tsaturyan A, Padrón R (2017) Lessons from a tarantula: new insights into muscle thick filament and myosin interacting-heads motif structure and function. Biophys Rev 9(5):461–480. https://doi.org/10.1007/s12551-017-0295-1

Alamo L, Pinto A, Sulbarán G, Mavárez J, Padrón R (2018) Lessons from a tarantula: new insights into myosin interacting-heads motif evolution and its implications on disease. Biophys Rev 10(5):1465–1477. https://doi.org/10.1007/s12551-017-0292-4

Bowslaugh J, Gittings W, Vandenboom R (2016) Myosin light chain phosphorylation is required for peak power output of mouse fast skeletal muscle in vitro. Pflugers Arch 468(11–12):2007–2016. https://doi.org/10.1007/s00424-016-1897-3

Bunda J, Gittings W, Vandenboom R (2018) Myosin phosphorylation improves contractile economy of mouse fast skeletal muscle during staircase potentiation. J Exp Biol. https://doi.org/10.1242/jeb.167718

Close R, Hoh JFY (1968) The after-effects of repetitive stimulation on the isometric twitch contraction of rat fast skeletal muscle. J Physiol. https://doi.org/10.1113/jphysiol.1968.sp008570

de Tombe PP, ter Keurs HEDJ (2016) Cardiac muscle mechanics: sarcomere length matters. J Mol Cell Cardiol 91:148–150. https://doi.org/10.1016/j.yjmcc.2015.12.006

de Tombe PP, Mateja RD, Tachampa K, Mou YA, Farman GP, Irving TC (2010) Myofilament length dependent activation. J Mol Cell Cardiol 48(5):851–858. https://doi.org/10.1016/j.yjmcc.2009.12.017

Dutka TL, Mollica JP, Lamboley CR, Weerakkody VC, Greening DW, Posterino GS, Murphy RM, Lamb GD (2017) S-nitrosylation and S-glutathionylation of Cys134 on troponin I have opposing competitive actions on Ca^{2+} sensitivity in rat fast-twitch muscle fibers. Am J Physiol Cell Physiol 312(3):C316–C327. https://doi.org/10.1152/ajpcell.00334.2016

Fillion M, Tiidus PM, Vandenboom R (2019) Lack of influence of estrogen on myosin phosphorylation and post-tetanic potentiation in muscles from young adult C57BL mice. Can J Physiol Pharmacol 97(8):729–737. https://doi.org/10.1139/cjpp-2018-0575

Fusi L, Brunello E, Yan Z, Irving M (2016) Thick filament mechano-sensing is a calcium-independent regulatory mechanism in skeletal muscle. Nat Commun 7:1–9. https://doi.org/10.1038/ncomms13281

Gittings W, Huang J, Smith IC, Quadrilatero J, Vandenboom R (2011) The effect of skeletal myosin light chain kinase gene ablation on the fatigability of mouse fast muscle. J Musc Res Cell Mot 31(5–6):337–348. https://doi.org/10.1007/s10974-011-9239-8

Gittings W, Bunda J, Stull JT, Vandenboom R (2016) Interaction of posttetanic potentiation and the catchlike property in mouse skeletal muscle. Muscle Nerve 54:308–316. https://doi.org/10.1002/mus.25053

Gittings W, Bunda J, Vandenboom R (2017) Shortening speed dependent force potentiation is attenuated but not eliminated in skeletal muscles without myosin phosphorylation. J Musc Res Cell Mot 38(2):157–162. https://doi.org/10.1007/s10974-017-9465-9

Gittings W, Bunda J, Vandenboom R (2018) Myosin phosphorylation potentiates steady-state work output without altering contractile economy of mouse fast skeletal muscles. J Exp Biol. https://doi.org/10.1242/jeb.167742

Gordon AM, Homsher E, Regnier M (2000) Regulation of contraction in striated muscle. Physiol Rev 80(2):853–924. https://doi.org/10.1152/physrev.2000.80.2.853

Houdusse A, Sweeney HL (2016) How myosin generates force on actin filaments. Trends Biochem Sci 41(12):989–997. https://doi.org/10.1016/j.tibs.2016.09.006

Irving M (2017) Regulation of contraction by the thick filaments in skeletal muscle. Biophys J 113(12):2579–2594. https://doi.org/10.1016/j.bpj.2017.09.037

Lehman W (2016) Thin filament structure and the steric blocking model. Compr Physiol 6(2):1043–1069. https://doi.org/10.1002/cphy.c150030

Levine RJC, Kensler RW, Yang Z, Stull JT, Sweeney HL (1996) Myosin light chain phosphorylation affects the structure of rabbit skeletal muscle thick filaments. Biophys J 71(2):898–907. https://doi.org/10.1016/S0006-3495(96)79293-7

Linari M, Brunello E, Reconditi M, Fusi L, Caremani M, Narayanan T, Piazzesi G, Lombardi V, Irving M (2015) Force generation by skeletal muscle is controlled by mechanosensing in myosin filaments. Nature 528:276–279. https://doi.org/10.1038/nature15727

Li Y, Lang P, Linke WA (2016) Titin stiffness modifies the force-generating region of muscle sarcomeres. Sci Rep 6:1–9. https://doi.org/10.1038/srep24492

MacDougall KB, Kristensen AM, MacIntosh BR (2020) Additional in-series compliance does not affect the length dependence of activation in rat medial gastrocnemius. Exp Physiol 105:1907–1917. https://doi.org/10.1113/EP088940

MacIntosh BR (2010) Cellular and whole muscle studies of activity dependent potentiation. In: Rassier D (ed) Muscle biophysics. Advances in experimental medicine and biology, vol 682. Springer, New York, pp 315–342. https://doi.org/10.1007/978-1-4419-6366-6_18

MacIntosh BR (2017) Recent developments in understanding the length dependence of contractile response of skeletal muscle. Eur J Appl Physiol 117(6):1059–1071. https://doi.org/10.1007/s00421-017-3591-3

MacIntosh BR, MacNaughton MB (2005) The length dependence of muscle active force: considerations for parallel elastic properties. J Appl Physiol 98(5):1666–1673. https://doi.org/10.1152/japplphysiol.01045.2004

Mateja RD, Greaser ML, de Tombe PP (2013) Impact of titin isoform on length dependent activation and cross-bridge cycling kinetics in rat skeletal muscle. Biochim Biophys Acta Mol Cell Res 1833:804–811. https://doi.org/10.1016/j.bbamcr.2012.08.011

Metzger JM, Greaser ML, Moss RL (1989) Variations in cross-bridge attachment rate and tension with phosphorylation of myosin in mammalian skinned skeletal muscle fibers: implications for twitch potentiation in intact muscle. J Gen Physiol 93(5):855–883. https://doi.org/10.1085/jgp.93.5.855

Millman BM (1998) The filament lattice of striated muscle. Physiol Rev 78(2):359–391. https://doi.org/10.1152/physrev.1998.78.2.359

Mollica JP, Dutka TL, Merry TL, Lamboley CR, Mcconell GK, Mckenna MJ, Murphy RM, Lamb GD (2012) S -Glutathionylation of troponin I (fast) increases contractile apparatus Ca^{2+} sensitivity in fast-twitch muscle fibres of rats and humans. J Physiol 590:1443–1463. https://doi.org/10.1113/jphysiol.2011.224535

Moore RL, Persechini A (1990) Length-dependence of isometric twitch tension potentiation and myosin phosphorylation in mouse skeletal muscle. J Cell Physiol 143:257–262. https://doi.org/10.1002/jcp.1041430209

Morris SR, Gittings W, Vandenboom R (2018) Epinephrine augments posttetanic potentiation in mouse skeletal muscle with and without myosin phosphorylation. Physiol Rep 6(9):1–13. https://doi.org/10.14814/phy2.13690

Overgaard K, Gittings W, Vandenboom R (2022) Potentiation of force by extracellular potassium and posttetanic potentiation are additive in mouse fast-twitch muscle in vitro. Pflugers Arch. https://doi.org/10.1007/s00424-022-02681-z

Persechini A, Stull JT, Cooke R (1985) The Effect of Myosin Phosphorylation on the Contractile Properties of Skinned Rabbit Skeletal Muscle Fibers. J Biol Chem 260(13):7951–7954. https://doi.org/10.1016/S0021-9258(17)39544-3

Rassier DR, Herzog W (2002) Effects of pH on the length-dependent twitch potentiation in skeletal muscle. J Appl Physiol 92:1293–1299. https://doi.org/10.1152/japplphysiol.00912.2001

Rassier DE, MacIntosh BR (2000) Length dependence of staircase potentiation: interactions with caffeine and dantrolene sodium. Can J Physiol Pharmacol 78(4):350–357. https://doi.org/10.1139/y99-143

Rassier DE, Macintosh BR (2002) Sarcomere length-dependence of activity-dependent twitch potentiation in mouse skeletal muscle. BMC Physiol 8:1–8

Rassier DE, MacIntosh BR (2002) Length-dependent twitch contractile characteristics of skeletal muscle. Can J Physiol Pharmacol 80(10):993–1000. https://doi.org/10.1139/y02-127

Rassier DE, Minozzo FC (2016) Length-dependent Ca^{2+} activation in skeletal muscle fibers from mammalians. Am J Physiol Cell Physiol 311(2):C201–C211. https://doi.org/10.1152/ajpcell.00046.2016

Rassier DE, Tubman LA, MacIntosh BR (1997) Length-dependent potentiation and myosin light chain phosphorylation in rat gastrocnemius muscle. Am J Physiol Cell Physiol 273(1):C198–C204. https://doi.org/10.1152/ajpcell.1997.273.1.c198

Rassier DE, Tubman LA, MacIntosh BR (1998) Caffeine and length dependence of staircase potentiation in skeletal muscle. Can J Physiol Pharmacol 76(10–11):975–982. https://doi.org/10.1139/y98-117

Rassier DE, MacIntosh BR, Herzog W (1999) Length dependence of active force production in skeletal muscle. J Appl Physiol 86(5):1445–1457. https://doi.org/10.1152/jappl.1999.86.5.1445

Reconditi M, Brunello E, Fusi L, Linari M, Martinez MF, Lombardi V, Irving M, Piazzesi G (2014) Sarcomere-length dependence of myosin filament structure in skeletal muscle fibres of the frog. J Physiol 592(5):1119–1137. https://doi.org/10.1113/jphysiol.2013.267849

Smith IC, Gittings W, Huang J, McMillan EM, Quadrilatero J, Tupling RR, Vandenboom R (2013) Potentiation in mouse lumbrical muscle without myosin light chain phosphorylation: is resting calcium responsible? J Gen Physiol 141(3):297–308. https://doi.org/10.1085/jgp.201210918

Smith IC, Vandenboom R, Tupling AR (2014) Juxtaposition of the changes in intracellular calcium and force during staircase potentiation at 30 and 37°C. J Gen Physiol 144(6):561–570. https://doi.org/10.1085/jgp.201411257

Stephenson GMM, Stephenson DG (1993) Endogenous MLC2 phosphorylation and Ca^{2+}-activated force in mechanically skinned skeletal muscle fibres of the rat. Pflugers Arch 424(1):30–38. https://doi.org/10.1007/BF00375099

Stull JT, Kamm KE, Vandenboom R (2011) Myosin light chain kinase and the role of myosin light chain phosphorylation in skeletal muscle. Arch Biochem Biophys 510(2):120–128. https://doi.org/10.1016/j.abb.2011.01.017

Sweeney HL, Houdusse A (2010) Structural and functional insights into the myosin motor mechanism. Annu Rev Biophys 39(1):539–557. https://doi.org/10.1146/annurev.biophys.050708.133751

Sweeney HL, Stull JT (1986) Phosphorylation of myosin in permeabilized mammalian cardiac and skeletal muscle cells. Am J Physiol Cell Physiol 250:4. https://doi.org/10.1152/ajpcell.1986.250.4.c657

Sweeney HL, Stull JT (1990) Alteration of cross-bridge kinetics by myosin light chain phosphorylation in rabbit skeletal muscle: implications for regulation of actin-myosin interaction. Proc Natl Acad Sci USA 87(1):414–418. https://doi.org/10.1073/pnas.87.1.414

Sweeney HL, Bowman BF, Stull JT (1993) Myosin light chain phosphorylation in vertebrate striated muscle: regulation and function. Am J Physiol Cell Physiol 264(5):C1085-1095. https://doi.org/10.1152/ajpcell.1993.264.5.c1085

Szczesna D, Zhao J, Jones M, Zhi G, Stull J, Potter JD (2002) Phosphorylation of the regulatory light chains of myosin affects Ca^{2+} sensitivity of skeletal muscle contraction. J Appl Physiol 92(4):1661–1670. https://doi.org/10.1152/japplphysiol.00858.2001

Vandenboom R (2017) Modulation of skeletal muscle contraction by myosin phosphorylation. Compr Physiol 7(1):171–212. https://doi.org/10.1002/cphy.c150044

Vandenboom R, Grange RW, Houston ME (1995) Myosin phosphorylation enhances rate of force development in fast-twitch skeletal muscle. Am J Physiol 268:596–603. https://doi.org/10.1152/ajpcell.1995.268.3.C596

Vandenboom R, Xeni J, Bestic M, Houston ME (1997) Increased force development rates of fatigued skeletal muscle are graded to myosin light chain phosphate content. Am J Physiol 272:1980–1984. https://doi.org/10.1152/ajpregu.1997.272.6.R1980

Wallinga-De Jonge W, Boom HBK, Boon KL (1980) Force development of fast and slow skeletal muscle at different muscle lengths. Am J Physiol Cell Physiol 8:6. https://doi.org/10.1152/ajpcell.1980.239.3.c98

Williams C, Regnier M, Daniel TL (2010) Axial and radial forces of cross-bridges depend on lattice spacing. PLoS Comput Biol. https://doi.org/10.1371/journal.pcbi.1001018

Williams CD, Salcedo MK, Irving TC, Regnier M, Daniel TL (2013) The length-tension curve in muscle depends on lattice spacing. Proc R Soc B 280:1766. https://doi.org/10.1098/rspb.2013.0697

Woodhead JL, Craig R (2015) Through thick and thin: interfilament communication in muscle. Biophys J 109(4):665–667. https://doi.org/10.1016/j.bpj.2015.07.019

Yamaguchi M, Kimura M, Li ZB, Ohno T, Takemori S, Hoh JFY, Yagi N (2016) X-ray diffraction analysis of the effects of myosin regulatory light chain phosphorylation and butanedione monoxime on skinned skeletal muscle fibers. Am J Physiol Cell Physiol 310(8):C692–C700. https://doi.org/10.1152/ajpcell.00318.2015

Yang Z, Stull JT, Levine RJC, Sweeney HL (1998) Changes in interfilament spacing mimic the effects of myosin regulatory light

chain phosphorylation in rabbit psoas fibers. J Struct Biol 122(1–2):139–148. https://doi.org/10.1006/jsbi.1998.3979

Zhang X, Kampourakis T, Yan Z, Sevrieva I, Irving M, Sun YB (2017) Distinct contributions of the thin and thick filaments to length-dependent activation in heart muscle. Elife 6:1–16. https://doi.org/10.7554/eLife.24081

Zhi G, Ryder JW, Huang J, Ding P, Chen Y, Zhao Y, Kamm KE, Stull JT (2005) Myosin light chain kinase and myosin phosphorylation effect frequency-dependent potentiation of skeletal muscle contraction. Proc Natl Acad Sci USA 102(48):17519–17524. https://doi.org/10.1073/pnas.0506846102